Optimal Expansion Planning of Energy Hub With Multiple Energy Infrastructures

Xiaping Zhang, Mohammad Shahidehpour, *Fellow, IEEE*, Ahmed Alabdulwahab, and Abdullah Abusorrah

***Abstract*—This paper presents an optimal expansion planning model for an energy hub with multiple energy systems. Energy hub represents a coupling among various energy infrastructures for supplying electricity, natural gas, and heating loads. Combined heat and power (CHP) and natural gas furnaces are considered within the energy hub to convert energy into other forms. The multiple energy system planning problem would optimally determine appropriate investment candidates for generating units, transmission lines, natural gas furnaces, and CHPs that satisfy electricity and heating load forecasts and hub system constraints. The system performances associated with reliability, energy efficiency, and emission matrices is evaluated for the identified planning schedules. Numerical simulations demonstrate the effectiveness of the proposed multiple energy system expansion planning approach based on energy hub.**

***Index Terms*—Combined heat and power (CHP), energy hubs, expansion planning, multiple energy systems (electricity, natural gas, heat).**

NOMENCLATURE

Indices

b	Index for load blocks.
h	Index for period.
t	Index for years.
i	Index for generating units.
l	Index for transmission line.
f	Index for natural gas furnace.
c	Index for combined heat and power (CHP).
m	Index for bus.
n	Index for ending bus of line l.
sp	Index of natural gas suppliers.
p	Index of natural gas pipelines.

Sets

EG	Set of existing generating units.
EL	Set of existing transmission lines.
EF	Set of existing natural gas furnaces.
CG	Set of candidate generating units.
CL	Set of candidate transmission lines.
CF	Set of candidate natural gas furnaces.
CC	Set of candidate CHP.

Parameters

DT	Duration time, in hour.
L	Energy output within energy hub, in MW/MMBtu.
R	System spinning reserve requirement, in MW.
PD	Forecasted electricity peak demand, in MW.
$P^{\max}$	Generation unit capacity, in MW.
$H^{\max}$	Thermal generation capacity, in MMBtu.
T	Number of years in the scheduling horizon.
T^{com}	Commissioning year.
x	Reactance of line.
d	Discount rate.
τ	Present-worth coefficient.
γ	Salvage factor.
η	Energy conversion efficiency.
κ	Dispatch factor.
GIC	Investment cost of generating unit.
TIC	Investment cost of transmission line.
FIC	Investment cost of natural gas furnace.
HIC	Investment cost of CHP.
VOLL	Value of lost load, in \$/MWh.
A	Hub-unit incidence matrix.
B	Hub-natural gas supplier load incidence matrix.
S^E	Hub-electricity branch connectivity matrix.
S^G	Hub-natural gas pipeline connectivity matrix.
C^E	Coupling matrix of electricity.
C^T	Coupling matrix of heat.

Variables

GC	Investment and operation cost of generating unit.
TC	Investment cost of transmission line.
FC	Investment cost of natural gas furnace.
HC	Investment cost of CHP.
OC	Operation cost.
DL	Curtailed electricity load, in MW.
E	Energy input within a hub, in MW/MMBtu.
P	Generation unit dispatch, in MW.
H	Thermal generation, in MMBtu.
y	Investment state of transmission line.
Z	Investment state of generating unit.
X	Investment state of natural gas furnace.

Manuscript received July 14, 2014; revised November 5, 2014; accepted January 6, 2015. This work was supported by the Deanship of Scientific Research (DSR) at King Abdulaziz University, Saudi Arabia, under Grant 8-135-35-RG. Paper no. TSG-00718-2014.

X. Zhang is with the Galvin Center for Electricity Innovation, Illinois Institute of Technology, Chicago, IL 60616 USA.

M. Shahidehpour is with the Galvin Center for Electricity Innovation, Illinois Institute of Technology, Chicago, IL 60616 USA, and also with the Renewable Energy Research Group, King Abdulaziz University, Jeddah 21589, Saudi Arabia (e-mail: ms@iit.edu).

A. Alabdulwahab and A. Abusorrah are with the Renewable Energy Research Group, King Abdulaziz University, Jeddah 21589, Saudi Arabia.

Color versions of one or more of the figures in this paper are available online at http://ieeexplore.ieee.org.

Digital Object Identifier 10.1109/TSG.2015.2390640

U	Investment state of CHP.
PL	Electricity branch flow.
θ	Electricity network bus angle.
F	Natural gas pipeline flow.
V	Gas delivery quantity of supplier, in MMBtu.
W	Total electric power generation, in MW.
Q_{th}	Total thermal power generation, in MMBtu.
Q_{fuel}	Total fuel input, in MMBtu.
EENS	Expected energy not served, in MWh.

I. Introduction

MOST FORMS of energy services are supplied by various independent infrastructures to industrial, commercial, and residential consumers. However, interdependencies of various energy infrastructures are significantly increased in recent years. The U.S. natural gas consumption by electric power sector has increased from 32% in 2007 to 39% in 2012 and the majority of new power generating capacity projected for the next decade is expected to utilize natural gas as its primary fuel [1]. In addition, there were nearly 70 gigawatts of CHP generating capacity spread across the U.S. accounting for almost 7% of total generation capacity [2]. The widespread utilization of the natural gas-fired generation and high efficient CHP units have affected the production, transmission, and distribution of various types of energy services including electricity, natural gas, and heat. Consequently, a comprehensive analysis for the optimal coordination of various energy systems is critical to the short-term operations and long-term planning of a sustainable energy supply.

A traditional expansion planning of energy infrastructures would determine the optimal size, location, and time for the addition of new resources over a planning horizon. Traditional planning strategies have often optimized one form of energy without considering its interactions with other types of energy systems. However, the issue is whether the use of traditional and separated planning tools would be sufficient for an efficient long-term planning of interdependent energy infrastructures. Additionally, synergies among various forms of energy are considered, with a new degree of freedom in energy supply, which represent a great opportunity for system improvements [3]. The co-optimization planning approach would functionally couple multiple energy infrastructures and enable exchanges among various energy infrastructures. In essence, the increased interdependency of various energy systems has offered an opportunity to optimize a holistic expansion planning approach which encompasses multiple energy infrastructures.

Traditionally, the resource expansion planning problem was concerned with one form of energy, e.g., electricity or natural gas. A market-based coordinated planning of electric power generation and transmission systems is proposed in [4]. Benders decomposition and Lagrangian relaxation methods are applied to simulate interactions among market participants and system operators in the planning process. An optimization method is introduced in [5] for enabling a long-term planning of natural gas networks with technical and economic conditions.

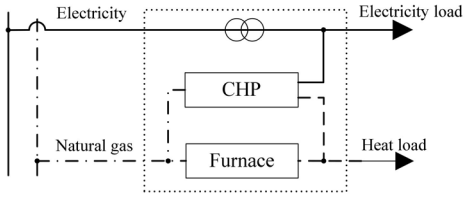

Fig. 1. Energy hub with electricity, natural gas, and heat systems.

Further studies were focused in recent years on the impact of interdependent operations of electricity and natural gas networks on power system security in [6]–[9]. The impact of natural gas infrastructure on the short-term operations of electric power system is discussed in [6]. The natural gas network is modeled by daily and hourly limits on pipelines, sub-areas, plants, and generating units in [7]. A steady-state natural gas network flow model is presented in [8] in order to analyze the impact of natural gas on the short-term unit commitment problem. A methodology for representing the natural gas supply, demand, and transportation network in the hydrothermal power system scheduling model is introduced in [9] to address the coordination between hydrothermal generation and natural gas.

The co-optimization modeling of multiple energy systems were addressed in several studies. A long-term multiarea generation/transmission expansion planning of integrated electricity and natural gas was presented in [10], which considered the natural gas value chain through pipelines from the supply to end-use consumers. An expansion planning model of an electricity and natural gas distribution system with high penetration of gas-fired distributed generation is presented in [11]. The conversion from one form of energy to another is not considered in the analysis of [10] and [11].

The energy hub concept is introduced in [12] to investigate combined economic dispatch and optimal power flow problems pertaining to the energy delivery. An energy hub represents an interface between energy participants (producers, consumers) and various energy system carriers [13], [14]. From a system point of view, an energy hub features input, output, conversion, and storage of multiple energy systems in a functional unit. Consider Fig. 1, which depicts an energy hub configuration for exchanging electricity, natural gas, and heat resources. The input hub port in Fig. 1 is connected to electricity and natural gas supplies. Inside the energy hub, multiple hardware devices for energy conversion are available including distribution transformers, CHPs, and natural gas furnaces. A CHP system could operate with a variety of fuels while the natural gas is the most common primary energy source. At the output port, hub electricity, and heating loads are supplied by multiple energy carriers.

The basic difference between an energy hub and a traditional energy system that interconnects natural gas and electric power components is that the loads within a hub can be supplied by multiple carriers for minimizing the total cost. Various energy carriers in a hub are characterized by their cost or availability, which offers several options for supplying the load. In Fig. 1,

the electricity load can be supplied either directly by electricity networks or by the CHP power generation using natural gas.

A few studies have addressed the interactions of various energy carriers in optimal energy hubs [15]–[18]. An approach in [15] considers the optimization of couplings (i.e., energy hub structure) among multiple energy networks consisting of electricity, natural gas, and district heating loads. A financial investment valuation method is proposed in [16] for energy hubs with conversion, storage, and demand-side management capabilities, which assesses the values added by the corresponding infrastructures. An integrated planning approach based on portfolio theory is discussed in [17], which calculates the optimal portfolio and relative shares of energy supplies. Moeini-Aghtaie *et al.* [18] aims to concentrate on the economic dispatch of multiple energy carriers at the presence of uncertain renewable energy resources.

We propose a long-term optimal expansion planning of an energy hub with multiple energy carriers including electricity, natural gas, and heat. Additionally, energy efficiency, emission, and reliability matrices are considered as evaluation criteria for the optimal planning. The objective is the least-cost planning of constrained energy infrastructures for satisfying the hub loads in the planning horizon. This consideration allows the energy conversion between various energy forms, which offers more flexibility to meet the future load requirement. The multiple energy planning problem is formulated to optimally determine appropriate candidates for generating units, transmission lines, natural gas furnaces, and CHPs which satisfy electricity and heating load forecasts and system constraints. The planning schedule is evaluated for its performance associated with reliability, energy efficiency, and emission matrices.

Energy hub represents an extension of a single energy carrier network. The energy hub planning model could be considered at different voltage levels because the large-scale resource planning is usually applied at the transmission level while the CHPs and gas heating loads are commonly located at the end-user side of distribution systems. So depending on its size, an energy hub could presumably encompass both transmission and distribution system voltage levels or reside explicitly at the distribution system level.

The rest of this paper is organized as follows. Section II introduces the typical energy hub architecture and discusses the general mathematical modeling. Section III presents the energy hub-based planning problem formulation and constraints. Section IV presents illustrative examples to show the proposed model applied to a practical power system. The conclusion drawn from this paper is provided in Section V.

II. Energy Hub Model

Consider a general energy hub with various energy carriers $\alpha, \beta, \ldots, \gamma$. Within the hub, energy is converted to various forms for meeting the load demand at the hub output port. The energy transfer from an input hub port to an output hub port is expressed as

$$\underbrace{\begin{pmatrix} L_\alpha \\ L_\beta \\ \vdots \\ L_\gamma \end{pmatrix}}_{L} = \underbrace{\begin{pmatrix} C_{\alpha\alpha} & C_{\beta\alpha} & \cdots & C_{\gamma\alpha} \\ C_{\alpha\beta} & C_{\beta\beta} & \ldots & C_{\gamma\beta} \\ \vdots & \vdots & \ddots & \vdots \\ C_{\alpha\gamma} & C_{\beta\gamma} & \cdots & C_{\gamma\gamma} \end{pmatrix}}_{C} \underbrace{\begin{pmatrix} E_\alpha \\ E_\beta \\ \vdots \\ E_\gamma \end{pmatrix}}_{E} \tag{1}$$

in which the energy at input and output ports are represented by $E = [E_\alpha, E_\beta, \ldots, E_\gamma]$ and $L = [L_\alpha, L_\beta, \ldots, L_\gamma]$, respectively. The matrix C is the forward coupling matrix which describes the conversion of energy from the input to the output. The elements of coupling matrix are coupling factors, which represents the converter efficiency and hub internal topology [19]. Consider a converter device for converting the α energy carrier into β with a coupling factor of $C_{\alpha\beta}$

$$L_\beta = C_{\alpha\beta} E_\alpha \tag{2}$$

where E_α and L_β denote energy input and output, respectively. For a single input-single output converter, the coupling factor corresponds to the converter's efficiency. The converter efficiency could be a variable as a function of operating point. As long as converter efficiency is fixed, the coupling matrix would represent a linear transformation of input energy to the output quantity.

In Fig. 1, the coupling matrix represents three converter devices: 1) transformer; 2) CHP plant; and 3) natural gas furnace. Here, the energy input vector E comprises electricity and natural gas

$$E = \begin{pmatrix} E_{el} \\ E_{\text{gas}} \end{pmatrix}. \tag{3}$$

The load demand vector L comprises electricity and heat

$$L = \begin{pmatrix} L_{el} \\ L_{\text{th}} \end{pmatrix}. \tag{4}$$

Input E and output L vectors are connected via efficiencies η of the conversion devices

$$L_{el} = \eta_{el} E_{el} + \eta_{ge}^{\text{CHP}} E_{\text{gas}}^{\text{CHP}} \tag{5}$$

$$L_{\text{th}} = \eta_{gth}^{\text{Fur}} E_{\text{gas}}^{\text{Fur}} + \eta_{gth}^{\text{CHP}} E_{\text{gas}}^{\text{CHP}} \tag{6}$$

$$E_{\text{gas}}^{\text{CHP}} = \kappa E_{\text{gas}} \tag{7}$$

$$E_{\text{gas}}^{\text{Fur}} = (1-\kappa) E_{\text{gas}} \tag{8}$$

where η_{el} denotes the electric transformer efficiency, η_{ge}^{CHP} and η_{gth}^{CHP} are the gas-electric and gas-thermal efficiencies of CHP, and η_{gth}^{Fur} is the efficiency of gas furnace. Additionally, a dispatch factor κ is introduced for natural gas, as natural gas is consumed by both CHP and natural gas furnace. Consequently, κE_{gas} of the natural gas consumption is converted to electricity and heat via CHP, and $(1-\kappa)E_{\text{gas}}$ of the gas consumption is used in the natural gas furnace to generate heat.

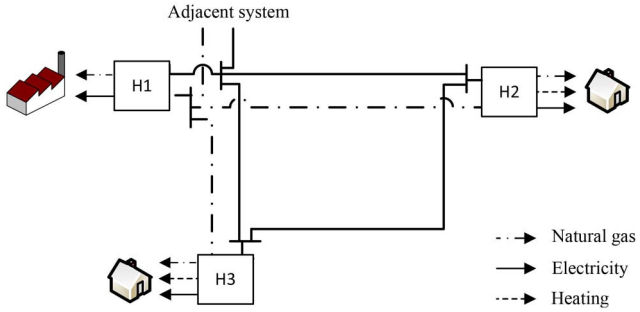

Fig. 2. Interconnected three-node energy hub system.

The efficiency and the dispatch factors together determine the coupling factor $C_{\alpha\beta}$. The conversion matrix is expressed as

$$\underbrace{\begin{pmatrix} L_{el} \\ L_{\text{th}} \end{pmatrix}}_{L} = \underbrace{\begin{pmatrix} \eta_{el} & \kappa\eta_{ge}^{\text{CHP}} \\ 0 & \kappa\eta_{gth}^{\text{CHP}} + (1-\kappa)\eta_{gth}^{\text{Fur}} \end{pmatrix}}_{C} \underbrace{\begin{pmatrix} E_{el} \\ E_{\text{gas}} \end{pmatrix}}_{E}. \quad (9)$$

In energy hubs, energy is supplied by coupled energy carriers. Fig. 2 shows an energy hub with three nodes (H1–H3) and three coupled networks for natural gas, electricity, and heat. The hub is tied to adjacent systems through its energy networks.

The energy input to the hub is distributed among hub nodes using the coupled hub networks as

$$\underbrace{\begin{pmatrix} E_{1\alpha} \\ \vdots \\ E_{i\alpha} \end{pmatrix}}_{E_\alpha} = \underbrace{\begin{pmatrix} s_{11} & \cdots & s_{1j} \\ \vdots & \ddots & \vdots \\ s_{i1} & \cdots & s_{ij} \end{pmatrix}}_{S_\alpha} \underbrace{\begin{pmatrix} fl_{1\alpha} \\ \vdots \\ fl_{j\alpha} \end{pmatrix}}_{F_\alpha} \quad (10)$$

where E_α shows hub inputs of energy carrier, S_α is a network connectivity matrix for carrier α with entries $\{0, +1, -1\}$, and F_α contains line flows of α.

III. Energy Hub Planning Model

A. Energy Hub Planning Objective

The objective of the proposed energy hub planning model is to minimize the total present value of the energy infrastructures including electricity, natural gas, and heat in the planning horizon (11). The objective includes the annual investment planning and operation costs associated with generating units, transmission lines, natural gas furnaces, and CHP plants, in addition to the cost of unserved energy. In (11), $\tau_t = 1/(1+d)^{t-1}$ is the present-worth coefficient of the resources at the end of the planning horizon, where d is discount rate.

The generation cost (12) includes the investment cost of new generating units and the operation cost of existing and new generating units. The investment cost of new generating units is a function of the capital cost and the unit capacity. The investment cost of new transmission lines is represented by (13). The salvage value represents the percentage of depreciation of the initial investment, which is included in the investment cost. For each installed resource, a higher salvage factor γ indicates a lower depreciation at the end of the planning horizon T.

The heating system cost (14) includes the investment cost of new gas furnace and the operation cost of existing and new natural gas furnaces. Equation (15) shows the investment and operation costs of new CHP plants. The cost of unserved energy is calculated by multiplying the expected energy not supplied (EENS) with the load shedding price for customers. The load shedding price is represented by the VOLL in \$/kWh

$$\text{Min} \sum_t \sum_{i\in\text{CG}} \tau_t \text{GC}_{it} + \sum_t \sum_{l\in\text{CL}} \tau_t \text{TC}_{lt} + \sum_t \sum_{f\in\text{CF}} \tau_t \text{FC}_{lt} + \sum_t \sum_{c\in CH} \tau_t \text{HC}_{\text{ct}} + \text{VOLL} \sum_t \tau_t \text{EENS}_t \quad (11)$$

$$\text{GC}_{it} = \text{GIC}_i P_i^{\max}\left(z_{it} - z_{i(t-1)}\right) - \frac{\tau_T}{\tau_t}\gamma_{it}\text{GIC}_i P_i^{\max}\left(z_{it} - z_{i(t-1)}\right) + \sum_h \sum_b \text{DT}_{bht}\text{OC}_i P_{\text{ibht}} \quad (12)$$

$$\text{TC}_{lt} = \text{TIC}_l\left(y_{lt} - y_{l(t-1)}\right) - \frac{\tau_T}{\tau_t}\gamma_{lt}\text{TIC}_l\left(y_{lt} - y_{l(t-1)}\right) \quad (13)$$

$$\text{FC}_{\text{ft}} = \text{FIC}_f\left(X_{\text{ft}} - X_{f(t-1)}\right) - \frac{\tau_T}{\tau_t}\gamma_{\text{ft}}\text{FIC}_f\left(X_{\text{ft}} - X_{f(t-1)}\right) + \sum_h \sum_b \text{DT}_{bht}\text{OC}_f H_{fbht} \quad (14)$$

$$\text{HC}_{\text{ct}} = \text{HIC}_c\left(U_{\text{ct}} - U_{c(t-1)}\right) - \frac{\tau_T}{\tau_t}\gamma_{\text{ct}}\text{HIC}_c\left(U_{\text{ct}} - U_{c(t-1)}\right) + \sum_h \sum_b \text{DT}_{bht}\text{OC}_c P_{cbht}. \quad (15)$$

B. System Planning Constraints

The energy hub planning problem which optimizes the investment plan for all candidate energy carrier systems is subject to commissioning time and installation constraints. A commissioning time is imposed on new installations (16)–(19). Once a candidate energy carrier is installed, its investment state will change to 1 for the remaining years (20)–(23). The annual electricity capacity planning constraint (24) requires that the candidate and existing units can collectively supply the forecasted peak demand and reserve capacity

$$z_{it} = 0 \quad \forall i \in \text{CG},\ \forall t < T_i^{\text{com}} \quad (16)$$

$$y_{lt} = 0 \quad \forall l \in \text{CL},\ \forall t < T_l^{\text{com}} \quad (17)$$

$$X_{\text{ft}} = 0 \quad \forall f \in \text{CF},\ \forall t < T_f^{\text{com}} \quad (18)$$

$$U_{\text{ct}} = 0 \quad \forall c \in CH,\ \forall t < T_c^{\text{com}} \quad (19)$$

$$z_{i(t-1)} \le z_{it} \quad \forall i \in \text{CG},\ \forall t \quad (20)$$

$$y_{l(t-1)} \le y_{lt} \quad \forall l \in \text{CL},\ \forall t \quad (21)$$

$$X_{f(t-1)} \le X_{\text{ft}} \quad \forall f \in \text{CF},\ \forall t \quad (22)$$

$$U_{c(t-1)} \le U_{\text{ct}} \quad \forall c \in CH,\ \forall t \quad (23)$$

$$\sum_{i\in\text{EG}} P_i^{\max} + \sum_{i\in\text{CG}} P_i^{\max} z_{it} + \sum_{i\in CH} P_c^{\max} U_{\text{ct}} \ge \text{PD}_{bht} + R_{bht} \quad \forall b,\ \forall h,\ \forall t. \quad (24)$$

C. Energy Hub System Constraints

For each node at the hub, the steady-state electricity and natural gas flow conservation is expressed as (25), (26), in which the sum of all branch flows is equal to the energy injection at the hub. S^E and S^G represent the connectivity matrix of electricity and natural gas networks respectively. PL and F denote the network flows of electricity and natural gas, respectively. The electricity and natural gas supplies are stated by P_{bht} and V_{bht} vectors. Within the energy hub, energy is converted through the coupling matrix (27), (28) to supply the load. The electric load is supplied by the imported power, local generation, or CHP. The heating load is either supplied by the natural gas furnace or CHP

$$E^{el}_{bht} = S^E * \mathrm{PL}_{bht} + \mathrm{A} * P_{bht} \quad \forall b,\ \forall h,\ \forall t \tag{25}$$
$$E^{\mathrm{gas}}_{bht} = S^G * F_{bht} + B * V_{bht} \quad \forall b,\ \forall h,\ \forall t \tag{26}$$
$$L^{el}_{bht} - \mathrm{DL}_{bht} = C^E * E^{el}_{bht} \quad \forall b,\ \forall h,\ \forall t \tag{27}$$
$$L^{\mathrm{th}}_{bht} = C^T * E^{\mathrm{gas}}_{bht} \quad \forall b,\ \forall h,\ \forall t. \tag{28}$$

The existing and candidate generating units are subject to capacity limits (29), (30). The electric and thermal power supplied by CHP is constrained by the unit capacity and the available natural gas flow (31)–(34). The thermal output of natural gas furnaces is subject to the capacity limits and the available natural gas (35)–(37)

$$0 \le P_{\mathrm{ibht}} \le P^{\max}_i \quad \forall i \in \mathrm{EG},\ \forall b,\ \forall h,\ \forall t \tag{29}$$
$$0 \le P_{\mathrm{ibht}} \le P^{\max}_i z_{it} \quad \forall i \in \mathrm{CG},\ \forall b,\ \forall h,\ \forall t \tag{30}$$
$$0 \le P_{cbht} \le P^{\max}_c U_{\mathrm{ct}} \quad \forall c \in \mathrm{CC},\ \forall b,\ \forall h,\ \forall t \tag{31}$$
$$0 \le H_{cbht} \le H^{\max}_c U_{\mathrm{ct}} \quad \forall c \in \mathrm{CC},\ \forall b,\ \forall h,\ \forall t \tag{32}$$
$$P_{cbht} = \kappa \eta^{\mathrm{CHP}}_{ge} E^{\mathrm{gas}}_{mbht} \quad \forall c \in \mathrm{CC},\ \forall b,\ \forall h,\ \forall t \tag{33}$$
$$H_{cbht} = \kappa \eta^{\mathrm{CHP}}_{gth} E^{\mathrm{gas}}_{mbht} \quad \forall c \in \mathrm{CC},\ \forall b,\ \forall h,\ \forall t \tag{34}$$
$$0 \le H_{fbht} \le H^{\max}_f \quad \forall f \in \mathrm{EF},\ \forall b,\ \forall h,\ \forall t \tag{35}$$
$$0 \le H_{fbht} \le H^{\max}_f X_{\mathrm{ft}} \quad \forall f \in \mathrm{CF},\ \forall b,\ \forall h,\ \forall t \tag{36}$$
$$H_{fbht} = (1-\kappa)\eta^{\mathrm{Fur}}_{gth} E^{\mathrm{gas}}_{mbht} \quad \forall f \in \mathrm{EF, CF},\ \forall b,\ \forall h,\ \forall t. \tag{37}$$

D. Transmission Network Flow Constraints

The network flow models incorporate the laws of the physics corresponding to the relations between voltage and current, gas pressure, and flow, etc. The characteristics of electricity and natural gas networks are discussed next.

1) Electricity Network Constraints: DC power flow is adopted in the planning model, representing a linear relation between line flows and bus phase angles. The existing and candidate line flows are modeled by (38)–(41). If the line is not installed, (40) is relaxed and (41) sets the line flow to zero. Once a line is installed, it will no longer be treated as a candidate. The voltage angle of the area incorporating slack bus is set to zero (42)

$$\mathrm{PL}_{lbht} = \frac{(\theta_{mbht} - \theta_{nbht})}{x_l} \quad \forall l \in \mathrm{EL},\ \forall b, \forall h, \forall t \tag{38}$$
$$|\mathrm{PL}_{lbht}| \le \mathrm{PL}^{\max}_l \quad \forall l \in \mathrm{EL}, \forall b, \forall h, \forall t \tag{39}$$
$$\left|\mathrm{PL}_{lbht} - \frac{(\theta_{mbht} - \theta_{nbht})}{x_l}\right| \le M(1-y_{lt}) \quad \forall l \in \mathrm{CL},\ \forall b, \forall h, \forall t \tag{40}$$
$$|\mathrm{PL}_{lbht}| \le \mathrm{PL}^{\max}_l y_{lt} \quad \forall l \in \mathrm{CL}, \forall b, \forall h, \forall t \tag{41}$$
$$\theta_{\mathrm{ref}} = 0. \tag{42}$$

2) Natural Gas Network Constraints: The natural gas transportation system consists of a complex network of pipelines, storage, and compressors which transport the natural gas from wellheads or suppliers to local distribution companies or directly to large commercial and industrial users [20]. Similar to the electric transmission lines which have a voltage limit for each bus, the natural gas network would maintain a guaranteed pressure at each node. The natural gas pipeline flow is driven by the pressure difference between two nodes, which is a nonlinear function of nodal pressure and natural gas pipeline characteristics. The nonlinear gas flow constrains make the feasible region of this problem nonconvex, and thus finding the global optimum cannot be guaranteed by numerical methods. Geidl and Andersson [12] applied a nonlinear programming software to provide a solution which may not be globally optimal. And the numerical methods may pose their limitations under certain system conditions. Liu *et al.* [8] solved the nonlinear distribution of natural gas flow by a fast forward substitution method, which used a large number of iterations and resulted in local optima. Both references are designed to handle a short-term dispatch problem, which requires a complex gas network model with an accurate estimation of natural gas network parameters. However, our long-term planning model uses a much longer time span with a larger problem size. Therefore, a linear natural gas network model is adopted, in this long-term planning problem, as a tradeoff between computation efficiency and modeling accuracy. Therefore, we consider the natural gas pipeline flow as a variable, which is constrained by the pipeline capacity at each period.

The natural gas flows along the pipeline are modeled by (43). Natural gas suppliers could be natural gas wells or storage facilities, which provides natural gas through its network. Supplies are modeled as positive gas injections at related nodes. The lower and upper limits of gas suppliers in each period are defined in (44). The consumption of natural gas furnaces and CHP units represent the natural gas load in the network and considered as negative gas injections at related nodes

$$f^{\min}_p \le f_p \le f^{\max}_p \quad \forall b,\ \forall h,\ \forall t \tag{43}$$
$$V^{\min}_{\mathrm{sp}} \le V_{\mathrm{sp}} \le V^{\max}_{\mathrm{sp}} \quad \forall b,\ \forall h,\ \forall t. \tag{44}$$

E. System Matrices Evaluation

Once the candidate carriers are identified by the energy hub planning problem, the performance of the planning schedule associated with reliability, energy efficiency, and carbon dioxide (CO_2) emission will be evaluated. The EENS is adopted as reliability index to measure the hub system reliability, when there is a loss-of-load. The annual EENS is calculated in (45), while the cost of unserved energy is included in the total planning cost represented by the objective function (11). Annual EENS limit is set for each year in the

entire planning horizon (46)

$$\text{EENS}_t = \sum_h \sum_b \text{DT}_{bht}\text{DL}_{bht} \quad \forall t \tag{45}$$

$$\text{EENS}_t \le \text{EENS}_t^{\text{limit}} \quad \forall t. \tag{46}$$

The overall system efficiency would measure what is produced (i.e., power and thermal output) as compared with what is consumed (i.e., fuel and power input) [21]. The overall system efficiency of the system (47) is calculated as the sum of the net useful electrical power output (W_E^{out}) and net useful thermal outputs (Q_{TH}) divided by the total fuel (Q_{FUEL}) and power input (W_E^{in}). The total input energy is determined by multiplying the fuel quantity by the heat rate of the fuel. Here, the natural gas volume is measured by its heat value in MMBtu; also 1 MW = 3.412 MMBtu for energy conversion

$$\eta_0 = \frac{W_E^{\text{out}} + Q_{\text{TH}}}{W_E^{\text{in}} + Q_{\text{FUEL}}}. \tag{47}$$

The environmental performance of the planned hub system is evaluated for the CO_2 emission since the combustion of natural gas releases very small amounts of sulfur dioxide and nitrogen oxides. For each device, the emission level is calculated based on the operating point, i.e., the dispatch of the unit and CHP or thermal generation of furnace. In this model, the energy efficiency and emission matrices are evaluated once the planning is scheduled, which would not incur any costs in the objective function.

F. Energy Hub Planning Methodology

We consider a linear energy hub topology characterized by a constant coupling matrix, which results in a linear conversion of various energies into linear constraints (25)–(28). Additionally, a linear energy flow network model is derived from dc power flow and simplified natural gas delivery equations. Therefore, (11)–(44) represent a convex mixed-integer linear programming problem, which is solved by commonly used optimization solver (e.g., CPLEX).

Fig. 3 depicts the flowchart of the proposed energy hub planning model. The input data consists of:

1) existing and candidate generating units, transmission network topology, and electrical load duration curve;
2) natural gas supplier and natural gas network topology;
3) existing and candidate natural gas furnaces, and heating load duration curve.

The input data are first processed to form the coupling and connectivity matrices of the multiple energy systems. Then, the energy hub planning optimization problem [see (11)–(44)] is solved for calculating the planning schedule, which provides the investment state of new facilities. The planning solution is checked by the annual reliability criterion. If the annual reliability limit is violated, a reliability constraint [see (46), (47)] is formed and added to the optimization problem. The iterative process is continued until an optimal planning schedule is obtained for satisfying the annual EENS_t criterion. At last, we calculate the system matrices associated with energy efficiency, CO_2 emission for evaluating the performance of the planning schedule, and dispatch.

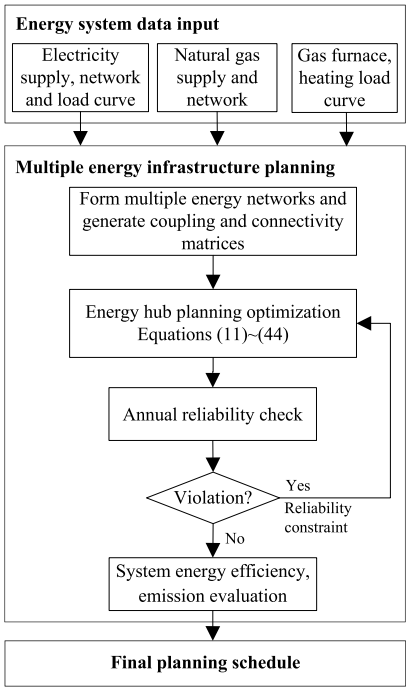

Fig. 3. Energy hub planning with multiple energy systems.

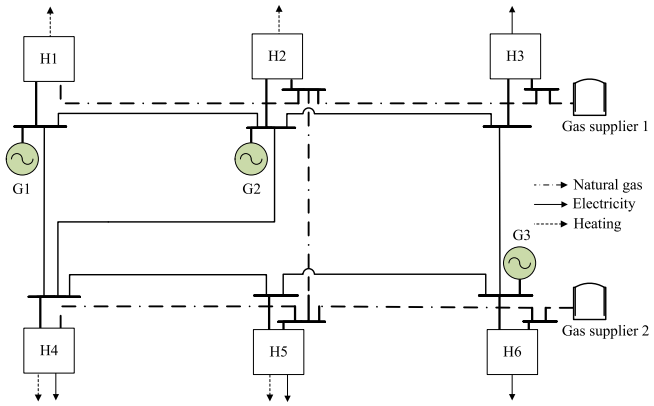

Fig. 4. Energy hub connected via electrical and natural gas networks.

IV. Case Studies

The proposed energy hub expansion planning model with a six-hub interconnected structure is illustrated in Fig. 4 with the existing and planned electricity and natural gas networks. The test data for the six-node multienergy hub are given in motor.ece.iit.edu/data/EnergyHubPlanning.xls.

The power system comprises six buses, three units, seven transmission lines, and three loads. A set of six candidate generating units, seven candidate transmission lines are considered. The natural gas/heating system is composed of six nodes, three natural gas furnaces, five pipelines, and two natural gas suppliers. Natural gas is supplied to feed the candidate combined heat plant and the gas furnace for heating loads. A set of four candidate natural gas furnaces and four CHP are considered to supply the loads in the planning horizon. Storage devices are not considered within the energy hub network in this planning model.

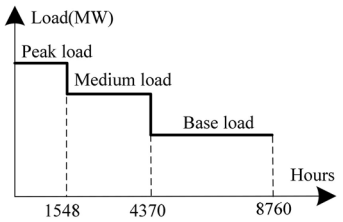

Fig. 5. Discretized load duration curve.

TABLE I
CANDIDATE UNIT CHARACTERISTICS AND INSTALLATION YEAR

Unit	Bus	Capacity (MW)	Comm. Year	Case 1	Case 2
1	1	8	3	*3*	-
2	2	10	4	-	*4*
3	3	6	6	*10*	-
4	4	8	5	-	-
5	5	10	6	-	-
6	6	8	8	-	-

TABLE II
CANDIDATE LINE CHARACTERISTICS AND INSTALLATION YEAR

Line	From bus	To Bus	Capacity (MW)	Comm. Year	Case 1	Case 2
1	1	2	15	5	-	-
2	2	3	10	2	-	-
3	1	4	10	4	*8*	-
4	2	4	10	6	-	*7*
5	4	5	10	5	-	-
6	5	6	10	3	-	-
7	3	6	10	2	-	-

TABLE III
CANDIDATE NATURAL GAS FURNACE CHARACTERISTICS AND INSTALLATION YEAR

Furnace	Node	Capacity (MMBtu)	Comm. Year	Case 1	Case 2
1	1	80	5	*6*	-
2	2	60	4	*4*	-
3	4	50	3	-	-
4	5	60	3	-	-

TABLE IV
CANDIDATE CHP PLANT CHARACTERISTICS AND INSTALLATION YEAR

CHP	Bus	Conversion efficiency	Capacity (MW)	Comm. Year	Case 1	Case 2
1	1	32% / 46%	16	2	-	*2*
2	2	31% / 45%	12	3	-	*4*
4	4	30% / 47%	12	2	-	-
5	5	33% / 44%	10	4	-	-

(η_{ge} / η_{gth} denote the gas-electric and gas-thermal efficiencies of the CHP.)

This paper is applied to a ten-year planning horizon and the investment costs are analyzed on an annual basis, i.e., each planned candidate resource is considered for installation at the beginning of each year. Each planning year is divided into 12 monthly periods. The monthly electricity load is divided into three load blocks representing base, medium, and peak loads as shown in Fig. 5. The quantity and the duration of load blocks may vary in each period within a year. The heating load which is highly correlated with weather profile is considered as a fixed quantity and a function of the average temperature in each period.

The planning analysis is implemented while the multiple energy infrastructure constraints are carried out for each load block. The initial electrical peak load is 29.8 MW with an average annual load growth rate of 3%. The natural gas-fired heating load has an average annual load growth rate of 0.8% with an initial peak load of 88.3 MMBtu. The discount rate is 5%. There are no limitations on annual investments or the number of components that can be installed in one year. The spinning reserve requirement is 5% of the load in each block [22]. The average VOLL is fixed at \$10/kWh.

Four cases are presented to illustrate the effectiveness of the energy hub-based planning for the multienergy infrastructures. The case study results are compared and analyzed based on investment cost, energy efficiency, emission, and reliability matrices.

Case 1: Decoupled planning of electricity and natural gas/heating systems in a hub.

Case 2: Hub planning with coupled multiple energy systems.

Case 3: Impact of CHP plant size in case 2.

Case 4: Impact of natural gas network transportation in case 2.

These cases are discussed as follows.

A. Case 1

The hub electricity and natural gas/heating systems are planned and operated in a decoupled mode in this case. Electric loads are supplied by generation units and heat is only generated by natural gas furnaces. The ten-year planning schedules of the two systems are presented in Tables I–IV. Tables I and II show the electric power system planning schedule in a hub with candidate units and lines. At the end of the planning horizon, 14 MW of new generation capacity at bus 1 and bus 3 and 1 transmission line from bus 1 to bus 4 are installed in order to meet the forecasted electricity load at a total planning cost of \$214.3 million. The load shedding occurs mainly at buses 3 and 4 between years 2 and 3 with a total EENS of 511 MWh and an unserved energy cost of \$5.1 million. We used an average VOLL of \$10/kWh for all the loads in this case, which is relatively low as compared to that of large commercial and industrial customers (usually is in a range of \$20–\$100/kWh). Therefore, the load shedding provides a viable and more economical option. In this case, the installation of new generation capacity at buses 3 or 4 can result in a higher total cost than the unserved energy cost. For the natural gas/heating systems system, two natural gas furnaces are installed at nodes 1 and 2 with a total planning cost of \$202.3 million as shown in Tables III and IV.

TABLE V
ECONOMIC COMPARISON OF PLANNING COSTS IN CASES 1 AND 2

Cost ($Million)		Case 1	Case 2
Investment Cost	Generation unit	9.051	6.289
	Transmission line	0.064	0.061
	Natural gas furnaces	23.35	-
	CHP	-	29.21
Operation cost	Electricity	200.0	373.4
	Heat	178.9	
Unserved electricity energy cost		5.110	0.514
Total planning cost		416.5	409.5

The total planning cost of the decoupled electricity and natural gas/heating systems to supply the increasing multiple loads at the hubs is $416.5 million in this case.

B. Case 2

We consider a coupled planning of electricity and natural gas/heating systems. In this case, 10 MW of new generation capacity at bus 2 and 1 transmission line from bus 2 to bus 4 are installed with a total investment cost $168.9 million for the electricity power system (i.e., lower than that in case 1). The natural gas furnaces are not installed in the planning horizon. However, two new CHP plants are scheduled in years 2 and 4, which can supply the increasing heating loads at nodes 1 and 2. Because of the electricity supply from the installed CHP plant, only one new conventional unit (G2) is installed at bus 2 in this case.

In Table V, the investment cost of case 2 is increased by $3.1 million because the average capital cost of CHP is higher than those of conventional generating units and natural gas furnaces. However, the CHP unit reduces the operation cost by $5.5 million as compared with that in case 1. This operation cost saving is mainly due to the utilization of a high efficient CHP plant which requires less fuel for producing energy than that considered in case 1. In addition, the load shedding only occurs at bus 4 in year 10 with a total unserved energy of 51.4 MWh. This feature would reduce the cost of unserved energy by $4.6 million compared with that in case 1. Therefore, the proposed coupled planning offers a compelling return on a slightly higher investment cost incurred in the planning horizon. This example supports the notion that total energy cost saving can be achieved as high efficiency CHPs are added to a hub for supplying electricity and heat. The proposed coupled planning of electricity and natural gas/heating systems offers considerable energy efficiency, environmental, and reliability benefits.

As shown in Fig. 6, the overall system efficiency is improved from 40.4% to 44.0% by adding a high efficiency CHP, which can capture a significant proportion of wasted heat through waste heat recovery technology. Compared with an average efficiency of 33% for fossil-fueled power plant, CHP typically can achieve 60%–80% efficiency by producing both electricity and thermal energy. The total emission in the planning horizon is reduced by 8.3% because CHP combusted less fuel than equivalent separate systems to produce the same amount of electricity and heat. The reliability performance is

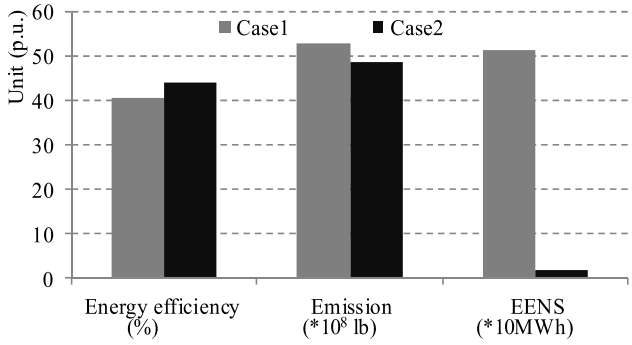

Fig. 6. Comparison of system matrices for cases 1 and 2.

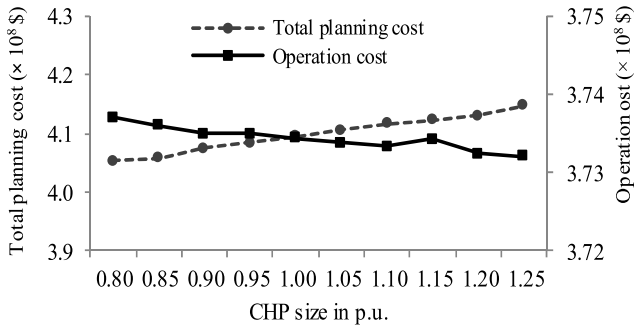

Fig. 7. Total planning and energy fuel cost versus CHP rating.

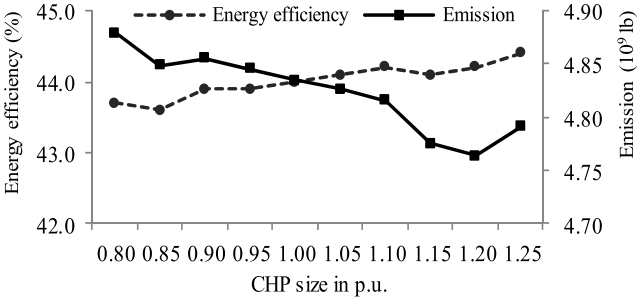

Fig. 8. System energy efficiency and emission versus CHP rating.

improved in this case with a lower EENS of 51.3 MWh as compared with the 511 MWh in case 1.

C. Case 3

We consider the impact of the CHP size on the investment cost and the system performance. The CHP capacity in case 2 corresponds to 1.0 per unit. The total planning cost shown in Fig. 7 increases, when we use a larger CHP because CHP has a fixed average capital cost that is higher than conventional gas-fired units. However, the increasing CHP capacity will result in a lower operation cost to supply the multiple loads. This is because less fuel is required to produce a given energy output than with separate heat and electricity power. More generation from larger size CHP would also bring improved energy efficiency and lower system emission as shown in Fig. 8.

However, increasing the CHP capacity beyond 1.25 per unit does not yield any more benefits because other restrictions on natural gas pipeline and electric transmission capacity would

TABLE VI
COMPARISON OF PLANNING COSTS AND SYSTEM PERFORMANCE

Cost ($Million)	Case 2	Case 4
Investment cost	35.59	37.33
Operation cost	373.4	371.4
Unserved electricity energy cost	0.513	-
Total planning cost	409.5	408.7
Energy efficiency (%)	44.01%	44.02%
Emission (10^8lb)	48.35	47.94
EENS (MWh)	51.3	-

limit the CHP merits. The newly installed CHP is located at nodes 1 and 2, which utilizes the available natural gas pipeline for transporting the fuel from natural gas suppliers located at nodes 3 and 6. Here, the pipeline with the smallest capacity, extending from node 2 to node 5, poses a bottleneck for connecting the two suppliers. So, the natural gas supplier 2 cannot provide any more fuel for supplying the additional CHP demand when this pipeline is fully loaded. In addition, the constrained transmission line capacity would limit the supply of cheaper CHP generation to other electrical loads. We consider a ten-year planning horizon in this particular example. However, proposed benefits pertaining to fuel cost saving, higher efficiency, and lower emission, which result from the utilization of high efficiency CHP, will be more prevalent in a longer planning horizon.

D. Case 4

In this case, we increase the natural gas pipeline capacity by 50% based on the reference value presented in case 2 and compare the planning solutions in Table VI. Here, the operation and the planning costs are lower by $2.0 and $0.8 million, respectively. In case 2, the pipeline capacity extending from node 2 to node 5 which linked two gas suppliers would limit the CHP fuel consumption at nodes 1 and 2. By contrast, the additional pipeline capacity in case 4 would supply a higher CHP power generation and thermal output as shown in Fig. 9. The increased natural gas pipeline capacity would increase the supply to conventional gas-fired generation units, for eliminating the unserved energy. In addition to improving the reliability performance, this case reduces the hub emission by 0.41×10^8 lb in the entire planning horizon. However, the energy efficiency does not change significantly because the loads supplied by CHP still represent a small portion of the total load (less than 20% of electricity load). This case indicates that the available transportation capacity in a hub would play a critical role in the coupled planning of multiple energy systems. Especially during natural gas peak demand periods (i.e., winter heating loads), both conventional gas-fired and CHP units could experience fuel supply variations since they largely rely on the real-time delivery of natural gas.

The proposed energy hub expansion planning model is solved using the ILOG CPLEX 11.0 in the general algebraic modeling system on an Intel Xeon Server with 64 GB RAM. The proposed model is a convex optimization problem which uses a linear energy hub topology and energy flow network model. We present a small system example to illustrate the proposed multiple energy system expansion planning method. The computation time for this small system is a few seconds. The proposed linear model can be easily applied to larger and more practical systems with an acceptable level of computational complexity.

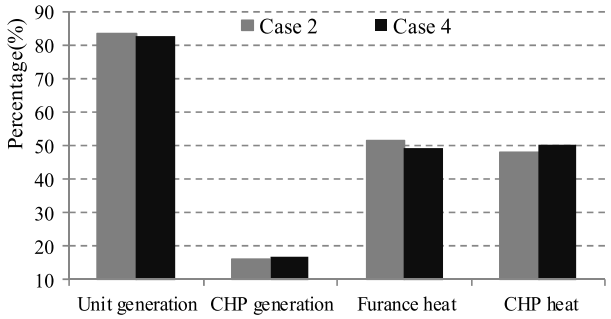

Fig. 9. Comparison of generation and heat distribution.

V. OBSERVATIONS

The specific features of the proposed energy hub planning model are summarized as follows.

1) The energy hub model would analyze interactions among electricity and natural gas/heating systems.
2) The energy hub offers opportunities to reduce operation costs and increase the overall energy efficiency by providing a certain degree of flexibility in energy supply.
3) The CHP capacity can impact the system performance because CHP is a critical element which links various energy systems for supplying electricity and heating loads.
4) The transportation capability of the energy transmission networks plays an important role in the energy hub planning since it greatly determines the energy flow to each hub node.

In this paper, we used a linear coupling matrix to link input and output energy quantities. The linear coupling would simplify the hub topology model and reduce the computational complexity of the planning problem. The introduction of energy storage devices could introduce additional challenges in the planning solution while enhancing the system performance associated with reliability, energy efficiency, and emissions. Our future work will be focused on improving the energy hub topology model. We will also consider a more practical converter efficiency as a function of operating point for hub devices.

VI. CONCLUSION

This paper proposed a long-term energy hub expansion planning model of electricity, natural gas, and heat systems in the planning horizon. A general energy hub model with multiple energy planning options was formulated along with constraints representing resource commission process, energy converting, and transmission networks. The energy hub planning model would determine the least-cost planning schedule of candidate generating units, transmission lines, natural gas furnaces, and CHPs that would satisfy electricity and heating loads.

The planning solution would be evaluated for demonstrating the hub performance associated with energy efficiency, emission, and reliability matrices. The proposed model was tested on a multiple energy system with six interconnected hubs. Case studies demonstrated that a coupled energy hub offers a more optimal schedule by providing a certain degree of flexibility for energy supply. The capacity of CHP would impact the system performance since the CHP supplies both the electricity and heating loads and provides a link for optimizing the various energy supply systems. Transmission network also plays a critical role as the energy flow relies on the transmission capacity. The proposed hub planning model can be used by system planners to calculate and evaluate energy efficiency as well as environmental and reliability performances by considering multiple energy system planning options in an energy hub.

ACKNOWLEDGMENT

The authors would like to thank the technical and financial support provided by the Deanship of Scientific Research (DSR), King Abdulaziz University, Jeddah, Saudi Arabia.

REFERENCES

[1] EIA. (2014). *Annual Energy Outlook*. [Online]. Available: http://www.eia.gov
[2] *Environmental Protection Agency*. [Online]. Available: http://www.epa.gov
[3] K. Hemmes, "Towards multi-source multi-product and other integrated energy system," *Int. J. Integr. Energy Syst.*, vol. 1, no. 1, pp. 1–15. Jan. 2009.
[4] J. H. Roh, M. Shahidehpour, and L. Wu, "Market-based generation and transmission planning with uncertainties," *IEEE Trans. Power Syst.*, vol. 24, no. 3, pp. 1587–1598, Aug. 2009.
[5] M. Hubner and H. Haubrich, "Long-term planning of natural gas networks," in *Proc. 5th Int. Conf. Eur. Elect. Market (EEM)*, Lisbon, Portugal, May 2008, pp. 1–5.
[6] M. Shahidehpour, Y. Fu, and T. Wiedman, "Impact of natural gas infrastructure on electric power systems," *Proc. IEEE*, vol. 93, no. 5, pp. 1042–1056, May 2005.
[7] T. Li, M. Eremia, and M. Shahidehpour, "Interdependency of natural gas network and power system security," *IEEE Trans. Power Syst.*, vol. 23, no. 4, pp. 1817–1824, Nov. 2008.
[8] C. Liu, M. Shahidehpour, Y. Fu, and Z. Li, "Security-constrained unit commitment with natural gas transmission constraints," *IEEE Trans. Power Syst.*, vol. 24, no. 3, pp. 1523–1535, Aug. 2009.
[9] B. Bezerra *et al.*, "Integrated electricity-gas operations planning in hydrothermal systems," in *Proc. X Symp. Special. Elect. Oper. Expansion (X SEPOPE)*, Florianópolis, Brazil, May 2006, pp. 1–9.
[10] C. Unsihuay, J. W. Marangon-Lima, A. C. Zambroni de Souza, I. Perez-Arriaga, and P. Balestrassi, "A model to long-term, multiarea, multistage and integrated expansion planning of electricity and natural gas systems," *IEEE Trans. Power Syst.*, vol. 25, no. 2, pp. 1154–1168, May 2010.
[11] C. Saldarriaga, R. Hincapie, and H. Salazar, "A holistic approach for planning natural gas and electricity distribution network," *IEEE Trans. Power Syst.*, vol. 28, no. 4, pp. 4052–4063, Nov. 2013.
[12] M. Geidl and G. Andersson, "Optimal power flow of multiple energy carriers," *IEEE Trans. Power Syst.*, vol. 22, no. 1, pp. 145–155, Feb. 2007.
[13] F. Kienzle, P. Favre-Perrod, M. Arnold, and G. Andersson, "Multi-energy delivery infrastructures for the future," in *Proc. Int. Conf. Infrastruct. Syst. Serv. Build. Netw. Brighter Future (INFRA)*, Rotterdam, The Netherlands, Nov. 2008, pp. 1–5.
[14] P. Favre-Perrod, F. Kienzle, and G. Andersson, "Modeling and design of future multi-energy generation and transmission systems," *Eur. Trans. Elect. Power*, vol. 20, no. 8, pp. 994–1008, Nov. 2010.
[15] M. Geidl and G. Andersson, "Operational and structural optimization of multi-carrier energy systems," *Eur. Trans. Elect. Power*, vol. 16, no. 5, pp. 463–477, 2006.
[16] F. Kienzle, P. Ahein, and G. Andersson, "Valuing investment in multi-energy conversion storage, and demand-side management systems under uncertainty," *IEEE Trans. Sustain. Energy*, vol. 2, no. 2, pp. 194–202, Apr. 2011.
[17] F. Adamek, M. Arnold, and G. Andersson, "On decisive storage parameters for minimizing energy supply costs in multicarrier energy systems," *IEEE Trans. Sustain. Energy*, vol. 5, no. 1, pp. 102–109, Jan. 2014.
[18] M. Moeini-Aghtaie, P. Dehghanian, M. Fotuhi-Firuzabad, and A. Abbaspour, "Multiagent genetic algorithm: An online probabilistic view on economic dispatch of energy hubs constrained by wind availability," *IEEE Trans. Sustain. Energy*, vol. 5, no. 2, pp. 699–708, Apr. 2014.
[19] M. Geidl, "Integrated modeling and optimization of multi-carrier energy systems," Ph.D. dissertation, Swiss Fed. Inst. Technol., ETH, Zurich, Switzerland, 2007.
[20] *Naturalgas.org*. [Online]. Available: http://www.naturalgas.org
[21] *American Council for an Energy-Efficient Economy*. [Online]. Available: http://www.aceee.org/
[22] NERC. (2011). *Operating Practices, Procedures, and Tools*. [Online]. Available: http://www.nerc.com/

Xiaping Zhang received the B.S. and M.S. degrees in electrical engineering from Shanghai Jiaotong University, Shanghai, China, in 2006 and 2009, respectively. She is currently pursuing the Ph.D. degree from the Illinois Institute of Technology, Chicago, IL, USA.

Mohammad Shahidehpour (F'01) is currently a Bodine Chair Professor and the Director of the Robert W. Galvin Center for Electricity Innovation, Illinois Institute of Technology, Chicago, IL, USA. He is also a Research Professor with the Renewable Energy Research Group, King Abdulaziz University, Jeddah, Saudi Arabia.

Dr. Shahidehpour was the recipient of the Honorary Doctorate from the Polytechnic University of Bucharest, Bucharest, Romania.

Ahmed Alabdulwahab received the Ph.D. degree in electrical engineering from the University of Saskatchewan, Saskatoon, SK, Canada, in 2003.

He is currently an Associate Professor with the Department of Electrical Engineering and Computer Engineering, and with the Renewable Energy Research Group, King Abdulaziz University, Jeddah, Saudi Arabia. He has been a Consultant at the Electricity and Co-Generation Regulatory Authority, Riyadh, Saudi Arabia, and a Visiting Scientist at Kinectrics and the University of Manchester, Manchester, U.K. His current research interests include power system planning and reliability evaluations.

Abdullah Abusorrah received the Ph.D. degree in electrical engineering from the University of Nottingham, Nottingham, U.K, in 2007.

He is an Associate Professor with the Department of Electrical Engineering and Computer Engineering, King Abdulaziz University, Jeddah, Saudi Arabia. He is the coordinator of the Renewable Energy Research Group and a member of the Energy Center Foundation Committee, King Abdulaziz University. His current research interests include power quality and system analyses.